THREE-DIMENSIONAL STABILITY ANALYSIS OF A RECTANGULAR PLATE IN AN AXIAL FLOW

Christophe Eloy & Lionel Schouveiler
IRPHE, CNRS & Aix-Marseille Université, Marseille, France

ABSTRACT

When immersed in an axial flow, a cantilevered plate can spontaneously exhibit flutter above a critical value of the flow velocity. If we suppose that there is no tensile effect (such as the gravity or the viscous stress) and that the viscoelastic damping in the elastic plate is negligible, this flag-type instability is entirely governed by three dimensionless parameters: the reduced flow velocity, the mass ratio and the aspect ratio of the plate. So far, the stability analysis found in the literature have assumed a two-dimensional problem corresponding to a plate of infinite span (Kornecki et al, 1976; Watanabe et al, 2002b). In the present study, we explicitly take into account the effect of the finite plate span.

1. INTRODUCTION

In his seminal paper on the instability of jets, Lord Rayleigh (1879) suggested that his theoretical approach could be used to show that an infinite flag is always unstable. Indeed, it can be proved easily that an elastic plate of infinite dimension (both in the span- and streamwise direction) is always unstable when immersed in an axial potential flow. However, this fluid-structure interaction problem becomes far more complex mathematically when the finite dimensions of the flag are explicitly taken into account.

Using analytical tools of airfoil theory, Kornecki et al (1976) have shown that a plate of infinite span but finite chord was stable for flow velocities below a critical velocity (in the following, we will use the term *plate* instead of *flag* to emphasise the importance of the finite density and finite bending stiffness of the material). Kornecki et al (1976) assumed an elastic plate and used two different theoretical approaches to model the flow around this plate. They first assumed a potential flow with zero circulation. Then, using a method introduced by Theodorsen (1935), they added a distribution of vorticity in the plate wake to smooth out the trailing edge singularity of the pressure field. This results in an unsteady circulatory flow. More recently these approaches have been used again with better computer accuracy (Huang, 1995; Watanabe et al, 2002b). Another theoretical approach has been used by Guo and Païdoussis (2000). They solved the two-dimensional problem (assuming infinite span) in the Fourier space for a potential flow.

An important aspect of these theoretical models is the way they deal with the flow at the boundary conditions. Kornecki et al (1976) in their zero-circulation model had pressure singularities both at the trailing and the leading edge. The use of the Theodorsen (1935) theory in the second model of Kornecki et al (1976) suppresses the trailing edge singularity by the use of the Kutta condition. In the theoretical model of Guo and Païdoussis (2000) the pressure distribution problem is solved in the Fourier space assuming implicitly no singularities. This means that an incoming "wake" has to be added to the flow to suppress the leading edge singularity. This "wake" cannot be justified on physical grounds.

Shayo (1980) first attempted a three-dimensional stability analysis to understand the dependence of the critical velocity on the plate span. In his study, he made several mathematical assumptions to simplify the calculation that led him to conclude that a flag of infinite span is more stable than a finite one. This latter result is in contradiction with a slender body approach (Lighthill, 1960; Datta and Gottenberg, 1975; Lemaitre et al, 2005).

Experiments with plates made of metal, paper or plastic sheets have been carried out by Taneda (1968), Datta and Gottenberg (1975), Kornecki et al (1976) and more recently by Yamaguchi et al (2000); Watanabe et al (2002a); Shelley et al (2005); Souilliez et al (2006) (see the book of Païdoussis, 2004, for a comprehensive list of references). These experiments showed that the flutter modes observed at threshold are always two-dimensional. They also showed that the instability threshold is always larger than the theoretical predictions. The work of Watanabe

et al (2002b) shows that the critical velocity measured in the experiments is at least twice as large as the analytical and numerical predictions for all experimental parameters. So far, no satisfactory explanation of this apparent discrepancy has been given.

Cantilevered plates in axial flow have also been modelled numerically by Watanabe et al (2002b), Tang et al (2003), Balint and Lucey (2005) and Tang and Païdoussis (2006). In these studies, a two-dimensional solver based on the Navier-Stokes equations or on a vortex method has been combined to a beam model for the plate. The critical velocities obtained with these numerical simulations are similar to the results of Kornecki et al (1976) and Guo and Païdoussis (2000).

In this paper, we present an analytical stability analysis of an elastic plate immersed in an axial uniform flow. The analysis assumes a one-dimensional flutter motion (as it has been observed in the experiments so far), but takes into account explicitly the finite span and chord of the plate to calculate the surrounding flow.

2. STABILITY ANALYSIS

2.1. Equation of motion

We consider a deformable rectangular plate, clamped at its leading edge and free at its side and trailing edges. The plate chord is L, its span H and its thickness h_p is assumed to be negligible in such a way that its flexural rigidity $D = Eh_p^3/12(1-\nu^2)$ remains finite (where E is the Young's modulus and ν the Poisson ration). As shown in Figure 1, the plate lies in the OXY plane and the wind of velocity U is parallel to OX. Assuming a one-dimensional deformation of the plate, its lateral deflection W is a function of the chord coordinate X and the time T only. For small deflection W, the dynamics obeys the linearised Euler-Bernoulli beam equation forced by the fluid load

$$m\frac{\partial^2 W}{\partial T^2} + D\frac{\partial^4 W}{\partial X^4} + \langle \delta P \rangle_Y = 0, \qquad (1)$$

where m is the mass per unit area of the plate $\delta P(X,Y)$ is the pressure difference between its two sides and $\langle . \rangle_Y$ denotes the average along the span for $-H/2 < Y < H/2$.

Equation (1) is valid as long as viscoelastic material damping and tension due to viscous stresses are negligible. The above equation is made dimensionless using $L/2$ as characteristic length along X and Z, $H/2$ as characteristic length

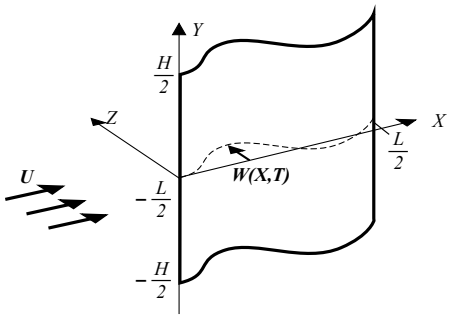

Figure 1: *Schematic of the plate subject to a one-dimensional deflection.*

along Y and U as characteristic velocity. Using lowercase letter for dimensionless quantities, we have

$$x = \frac{X}{2L}, \quad y = \frac{Y}{2H}, \quad w = \frac{W}{2L}, \quad t = \frac{2UT}{L}, \qquad (2)$$

and equation (1) becomes

$$\frac{\partial^2 w}{\partial t^2} + \frac{4}{U^*}\frac{\partial^4 w}{\partial x^4} + \frac{M^*}{2}\langle \delta p \rangle_y = 0, \qquad (3)$$

where p is the dimensionless pressure, U^* the reduced velocity and M^* the mass ratio given by

$$p = \frac{P}{\rho U^2}, \quad M^* = \frac{\rho L}{m}, \quad U^* = \sqrt{\frac{m}{D}}LU, \qquad (4)$$

with ρ the density of the surrounding fluid. Note that the problem is entirely governed by three dimensionless parameters: the critical velocity U^*, the mass ratio M^* and the plate aspect ratio

$$H^* = \frac{H}{L}. \qquad (5)$$

2.2. Galerkin decomposition

Equation of motion (1) becomes linear if p is linear with respect to w (this is the case if the flow is supposed to be potential). In this case, we can assume a Galerkin decomposition of the lateral deflection and switch to the frequency domain such that the deflection w can be written as

$$w(x,t) = \sum_{n=1}^{N} a_n w_n(x) \mathrm{e}^{\mathrm{i}\omega t} + \text{c.c.}, \qquad (6)$$

where c.c. denotes the complex conjugate, N is the truncation of the Galerkin expansion and w_n are the beam eigenfunctions *in vacuo* satisfying the free boundary-condition at the trailing edge and a clamped boundary-condition at the

leading edge (see Païdoussis, 1998, 2004). Note that these Galerkin modes satisfy the relation $w_n^{(4)} = k_n^4 w_n$, where k_n are wavenumbers sorted in ascending order.

To solve the equation of motion (1) using the Galerkin expansion (6), one needs to determine the pressure jump $\delta p_n(x,y)$ associated with the deflection $w_n(x)$ at angular frequency ω. This will be done in the next section.

Upon defining the standard scalar product as

$$f \otimes g = \frac{1}{2}\int_{-1}^{1} f(x)g(x)\mathrm{d}x, \tag{7}$$

the Galerkin modes satisfy the orthogonality condition $y_m \otimes y_n = \delta_m^n$, where δ_i^j is the Kronecker delta. By multiplying Eq. (1) by the modes w_m, the equation of motion becomes a system of N linear equations with N unknowns (the amplitudes a_n). The solvability condition imposes

$$\det\left(-\omega^2\mathcal{I} + \frac{4}{U^{*2}}\mathcal{Q} + \frac{M^*}{2}\mathcal{P}\right) = 0, \tag{8}$$

where $\mathcal{I}$ is the $N\times N$ identity matrix, $\mathcal{Q}$ is the diagonal matrix with the elements k_n^4 in ascending order on its diagonal and

$$\mathcal{P}_{mn}(\omega) = y_m \otimes \langle \delta p_n \rangle_y, \tag{9}$$

where p_n is the pressure field associated to the Galerkin mode w_n with same frequency dependence. Note that the matrix $\mathcal{P}$ is a function of ω as it will be shown below.

For a given mass ratio M^* and dimensionless velocity U^*, the solvability condition (8) has $2N$ solutions ω_i corresponding to each flutter mode. The frequencies of the flutter modes are simply given by $\Re(\omega_i)$ and their growth rates by $\sigma_i = -\Im(\omega_i)$. To determine the stability of the plate flutter, one now needs to calculate the matrix $\mathcal{P}$ and search the velocity U^* needed to have at least one flutter mode with a positive growth rate.

3. THREE-DIMENSIONAL FLOW

In the section, we follow the calculations and notations of Guermond (1990) and Guermond and Sellier (1991) done in the context of the lifting-line theory. The main difference comes from the fact that we are treating different limits.

3.1. Inverse problem

Assuming a potential flow, the pressure field is given by the linearized form of the Bernoulli law which in dimensionless form can be written as

$$p_n(x,y,z) = -\left(\mathrm{i}\omega + \frac{\partial}{\partial x}\right)\phi_n, \tag{10}$$

where $\phi_n(x,y,z)$ is the velocity potential at frequency ω. Provided the perturbation pressure vanishes at $x=-\infty$, the differential operator $(\mathrm{i}\omega + \partial/\partial x)$ can be inverted and gives

$$\phi_n = -\int_{-\infty}^{0} \mathrm{e}^{\mathrm{i}\omega v} p_n(x+v,y,z)\mathrm{d}v. \tag{11}$$

From these relations, it is evident that the problem can be formulated equivalently in terms of ϕ_n or p_n which are both potential fields. From a pratical point of view, the pressure formulation is better because it is continuous everywhere except across the plate and it allows to obtain directly the field seeked.

The pressure field satisfies the following equations

$$\Delta p_n = 0, \tag{12}$$

$$\frac{\partial p_n}{\partial z} = -\left(\mathrm{i}\omega + \frac{\partial}{\partial x}\right)^2 w_n \quad \text{on } S, \tag{13}$$

$$p_n = 0 \quad \text{at the trailing edge}, \tag{14}$$

$$p_n \to 0 \quad \text{at infinity}, \tag{15}$$

where the Laplace operator takes the following form because of the different scales in the spanwise and chordwise direction

$$\Delta = \frac{\partial^2}{\partial x^2} + \frac{1}{H^{*2}}\frac{\partial^2}{\partial y^2} + \frac{\partial^2}{\partial z^2}. \tag{16}$$

The Neumann boundary condition (13) on S the surface of the plate comes from the continuity of the normal velocity. Equation (14) is the Kutta condition and allows for a unique solution of the problem.

Using Green representation theorem and following Guermond and Sellier (1991), the deflection w_n and the pressure jump δp_n can be related

$$\int_{-\infty}^{0} \mathrm{e}^{\mathrm{i}\omega v} \iint_S \frac{\delta p_n(\xi,\eta)\,\mathrm{d}\xi\,\mathrm{d}\eta\,\mathrm{d}v}{\left[(x-\xi+v)^2 + H^{*2}(y-\eta)^2\right]^{3/2}} = -\frac{4\pi}{H^*}\left(\mathrm{i}\omega + \frac{\partial}{\partial x}\right) w_n, \tag{17}$$

for (x,y) on the surface of the plate S. Here, the surface integral as to be taken in the finite-part sense as introduced by Hadamard (1932) and summarized in Guermond (1990) or otherwise, the integral would diverge. The above equation

is a Fredholm equation of the first kind which has to be inverted in order to calculate the pressure jump δp_n. For a given aspect ratio H^*, this inversion can be accomplished numerically. In the present paper, we will detail an analytical inversion in the limit of a slender plate, i.e. $H^* \ll 1$.

3.2. Slender-body limit

In the limit of small aspect ratio, the inverse problem (17) can be simplified into

$$\left(\mathrm{i}\omega + \frac{\partial}{\partial x}\right)^2 w_n = \frac{1}{4\pi}\int_{-1}^{1} I(x,\epsilon)\,\mathrm{d}\eta, \qquad (18)$$

where

$$I(x,\epsilon) = \int_{-1}^{1} \frac{\gamma(\xi,\eta)}{(x-\xi)^2}\frac{\epsilon\,\mathrm{d}\xi}{[\epsilon^2+(x-\xi)^2]^{1/2}}, \qquad (19)$$

and

$$\gamma = -\frac{\partial \delta p_n}{\partial y}, \quad \epsilon = H^*(y-\eta) \ll 1. \qquad (20)$$

An expansion of $I(x,\epsilon)$ can be calculated in the limit of small ϵ using the method of matched asymptotic expansion. After some calculation, it gives

$$I(x,\epsilon) = -\frac{2}{\epsilon}\gamma(x,\eta) + \epsilon\ln 2\,\gamma''(x,\eta) + \epsilon\int_{-1}^{1}\frac{\gamma(\xi,\eta)\,\mathrm{d}\xi}{|x-\xi|^3} + O(\epsilon^3), \qquad (21)$$

where the prime denotes differentiation with respect to x and the integral has to be taken in the finite-part sense. Injecting this expansion into the integral equation (18) gives

$$\left(\mathrm{i}\omega + \frac{\partial}{\partial x}\right)^2 w_n = \frac{1}{4\pi}\int_{-1}^{1}\int_{-1}^{1}\gamma(\xi,\eta) \times K(x-\xi,y-\eta)\,\mathrm{d}\xi\,\mathrm{d}\eta, \qquad (22)$$

where K is the kernel of the Fredholm equation which can be expressed as an expansion in H^*

$$K(x,y) = -\frac{2\delta(x)}{H^* y} + H^*\ln 2\,\delta''(x)y + H^*\frac{y}{|x|^3} + O(H^{*3}), \qquad (23)$$

where $\delta(x)$ is the Dirac delta.

At first order in H^*, the solution of (22) is

$$\gamma_0 = 2H^*\frac{y}{\sqrt{1-y^2}}\left(\mathrm{i}\omega + \frac{\partial}{\partial x}\right)^2 w_n, \qquad (24)$$

which gives after y-integration and averaging

$$\langle \delta p_n^{(0)}\rangle_y = \frac{\pi H^*}{2}\left(\mathrm{i}\omega + \frac{\partial}{\partial x}\right)^2 w_n, \qquad (25)$$

as predicted by the slender-body theory of Lighthill (1960). The next order correction is found by injecting the above solution into (22) and gives

$$\langle \delta p_n^{(1)}\rangle_y = \frac{H^{*2}}{4}\left(\ln 2\langle \delta p_n^{(0)}\rangle_y'' + \int_{-1}^{1}\frac{\langle \delta p_n^{(0)}\rangle_y}{|x-\xi|^3}\mathrm{d}\xi\right), \qquad (26)$$

where again the last integral is taken in the finite-part sense. So the total average pressure jump takes the form

$$\langle \delta p_n\rangle_y = \langle \delta p_n^{(0)}\rangle_y + \langle \delta p_n^{(1)}\rangle_y + O(H^{*5}). \qquad (27)$$

The method described here can be carried out up to any order in H^* without difficulty.

4. CONCLUSION

The work presented here is still in progress. This explain why no quantitative results are presented at this moment. However, the method used here and inspired from lifting-line theory seems very promising and will probably help to gain knowledge in the flutter instability of plates or flags.

The present work will also help to clarify and validate the hypothesis made in the Fourier analysis of Eloy et al (2007) and whose main results are summarized in figure 2.

5. REFERENCES

Balint, T. S. and Lucey, A. D., 2005. Instability of a cantilevered flexible plate in viscous channel flow. *Journal of Fluids and Structures*, **20**: 893–912.

Datta, S. K. and Gottenberg, W. G., 1975. Instability of an elastic strip hanging in an airstream. *Journal of Applied Mechanics, Transactions of the ASME*, pages 195–198.

Eloy, C., Souilliez, C., and Schouveiler, L., 2007. Flutter of a rectangular plate. *Journal of Fluids and Structures*, **23**: 904–919.

Guermond, J.-L., 1990. A generalized lifting-line theory for curved and swept wings. *J. Fluid Mech.*, **211**: 497–513.

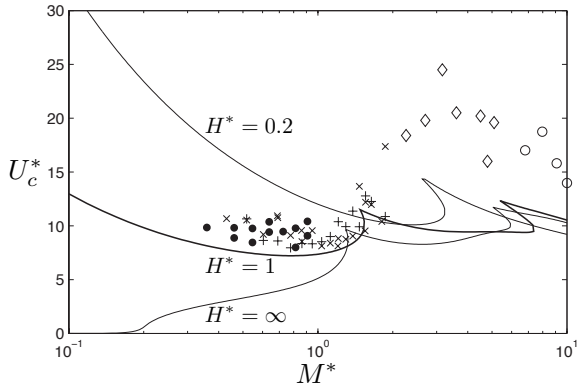

Figure 2: *Critical flow velocity as a function of the mass ratio of the plate. The different symbols correspond to experimental measurements for $H^* = 1$: crosses (Souilliez et al, 2006) and filled circles (Huang, 1995); and $H^* = 0.25$: open symbols (Yamaguchi et al, 2000). Lines correspond to theoretical prediction using a Fourier approach (Eloy et al, 2007) for different values of the aspect ratio as labelled.*

Guermond, J.-L. and Sellier, A., 1991. A unified unsteady lifting-line theory. *J. Fluid Mech.*, **229**: 427–451.

Guo, C. Q. and Païdoussis, M. P., 2000. Stability of rectangular plates with free side-edges in two-dimensional inviscid channel flow. *Journal of Applied Mechanics, Transactions of the ASME*, **67**: 171–176.

Hadamard, J., 1932. *Lectures on Cauchy's problem in linear differential equation*. Dover.

Huang, L., 1995. Flutter of cantilevered plates in axial flow. *Journal of Fluids and Structures*, **9**: 127–147.

Kornecki, A., Dowell, E. H., and O'Brien, J., 1976. On the aeroelastic instability of two-dimensional panels in uniform incompressible flow. *Journal of Sound and Vibration*, **47**(2): 163–178.

Lemaitre, C., Hémon, P., and de Langre, E., 2005. Instability of a long ribbon hanging in axial air flow. *Journal of Fluids and Structures*, **20**(7): 913–925.

Lighthill, M. J., 1960. Note on the swimming of slender fish. *J. Fluid Mech.*, **9**: 305–317.

Païdoussis, M. P., 1998. *Fluid-Structure Interactions: Slender Structures And Axial Flow, Volume 1*. Academic Press.

Païdoussis, M. P., 2004. *Fluid-Structure Interactions: Slender Structures And Axial Flow, Volume 2*. Elsevier Academic Press.

Rayleigh, L., 1879. On the instability of jets. *Proc. London Math. Soc.*, **X**: 4–13.

Shayo, L. W., 1980. The stability of cantilever panels in uniform incompressible flow. *Journal of Sound and Vibration*, **68**(3): 341–350.

Shelley, M., Vandenberghe, N., and Zhang, J., 2005. Heavy flags undergo spontaneous oscillations in flowing water. *Phys. Rev. Lett.*, **94**: 094302.

Souilliez, C., Schouveiler, L., and Eloy, C., 2006. An experimental study of flag flutter. *Proceeding of the 6th FSI, AE & FIV+N Symposium, ASME PVP 2006 / ICPVT-11 Conference*.

Taneda, S., 1968. Waving motions of flags. *Journal of the Physical Society of Japan*, **24**(2): 392–401.

Tang, D. M., Yamamoto, H., and Dowell, E. H., 2003. Flutter and limit cycle oscillations of two-dimensional panels in three-dimensional axial flow. *Journal of Fluids and Structures*, **17**: 225–242.

Tang, L. and Païdoussis, M. P., 2006. A numerical investigation on the dynamics of two-dimensional cantilevered flexible plates in axial flow. *Proceeding of the 6th FSI, AE & FIV+N Symposium, ASME PVP 2006 / ICPVT-11 Conference*.

Theodorsen, T., 1935. General theory of aerodynamic instability and the mechanism of flutter. *NACA Report 496*.

Watanabe, Y., Suzuki, S., Sugihara, M., and Sueoka, Y., 2002a. An experimental study of paper flutter. *Journal of Fluids and Structures*, **16**(4): 529–542.

Watanabe, Y., Isogai, K., Suzuki, S., and Sugihara, 2002b. A theoretical study of paper flutter. *Journal of Fluids and Structures*, **16**(4): 543–560.

Yamaguchi, N., Sekiguchi, T., Yokota, K., and Tsujimoto, Y., 2000. Flutter limits and behavior of a flexible thin sheet in high-speed flow - II: Experimental results and predicted behaviors for low mass ratios. *Transaction of the ASME Journal of Fluids Engineering*, **122**: 74–83.